Journal of Cardiovascular Magnetic Resonance (2006) **8,** 327–333

ISSN: 1097-6647 print / 1532-429X online
DOI: 10.1080/10976640500451903

Taylor & Francis
Taylor & Francis Group

MYOCARDIAL INFARCTION

CINE-MR Imaging of the Normal and Infarcted Rat Heart Using an 11.7 T Vertical Bore MR System

Damian J. Tyler,[1] Craig A. Lygate,[2] Jürgen E. Schneider,[2] Paul J. Cassidy,[1] Stefan Neubauer,[2] and Kieran Clarke[1]

Departments of Physiology[1] and Cardiovascular Medicine,[2] University of Oxford, Oxford, United Kingdom

ABSTRACT

MR imaging is uniquely placed to non-invasively study rodent cardiac structure and function. High-field MR scanners commonly have a vertical bore, and the purpose of this work was to demonstrate CINE-MR imaging in normal and infarcted rat hearts after determining hemodynamic stability when positioned vertically for imaging. Optimisation of imaging parameters was carried out prior to assessment of cardiac function in a group of normal and infarcted rat hearts.

Rat hemodynamics were unaltered when vertical for 90 minutes, compared with horizontal measurements and rat cardiac parameters were measured accurately and reproducibly with our optimized CINE-MR protocol. A flip angle of 17.5° was shown to provide optimal contrast for the assessment of structure and function, and, in contrast to our findings in mice, respiratory gating was not found to be essential. Hence, we conclude that vertical bore MR systems can be used to measure *in vivo* cardiac function in normal and infarcted rat hearts.

INTRODUCTION

Heart disease and subsequent heart failure is the greatest cause of mortality in the developed world (1, 2). Animal models, genetic models in mice, and other models in rats are key to the study of the cellular mechanisms leading to heart disease and allow the study of possible therapeutic interventions (3–9).

Magnetic resonance (MR) imaging enables the accurate evaluation of animal heart disease models (8, 10–12). High-resolution imaging provides measures of cardiovascular anatomy, and when combined with CINE imaging techniques, permits the investigation of cardiac functional parameters, such as ejection fraction and cardiac output (13). Also, the non-invasive nature of MR imaging is ideally suited for the longitudinal monitoring of the development of cardiac abnormalities and allows the structural and functional changes that occur in heart failure to be monitored (14).

Cardiac MR studies in rats have traditionally been performed using MR systems with horizontal bores and field strengths $\leq$7 T (11, 14, 15–26). However, experimental high-field MR systems are commonly built with a vertical bore, which is the preferred design for spectroscopic experiments in isolated, perfused organs (7). The higher magnetic field strength of such systems leads to an increased signal to noise ratio (SNR), which can improve spatial and temporal resolution or reduce total scan times, allowing greater throughput. For *in vivo* studies on vertical bore MR systems, animals have to be positioned in an upright position (head up), which may affect hemodynamics. There were no hemodynamic effects in mice placed in a vertical position for MR assessment for over an hour (27). However, the effect of placing a larger animal, such as the rat, in a vertical position is unknown, although it is thought that such a study in larger mammals and in humans would be impractical because orthostasis would reduce venous return, LV volumes and cardiac output (28).

Hemodynamic stability in vertically positioned rats would allow cardiovascular studies in high-field, vertical bore systems and would allow direct comparisons between structural

Keywords: Rat, MR-CINE Imaging, Gating, Cardiac Function, Myocardial Infarction.
This work was funded by the British Heart Foundation.
Correspondence to:
Dr. Damian Tyler, PhD
University Laboratory of Physiology,
University of Oxford,
Parks Road,
Oxford.
OX1 3PT
UK
phone ++44-1865-282 247; fax: ++44-1865-282 272
email: damian.tyler@phvsiol.ox.ac.uk

and functional data acquired in imaging experiments and spectroscopic information available from studies of *in vivo* or isolated perfused hearts. Consequently, we have determined whether rats are hemodynamically stable in a vertical position over 90 minutes, a time appropriate for a full MR assessment of cardiac structure and function. We implemented a CINE-MR protocol on an 11.7 T MR system with a vertical bore and investigated optimal acquisition parameters and physiological gating strategies. The MR protocol in normal Wistar rats provided CINE-MR images at a high spatial and temporal resolution. We have also studied Wistar rats after myocardial infarction to demonstrate the feasibility of the technique to study animals with abnormal cardiac function.

MATERIALS AND METHODS

Animals

All animals were obtained from a commercial breeder (Harlan, United Kingdom) and kept under controlled conditions for temperature, humidity and light, with chow and water available *ad libitum.* All investigations conformed to Home Office Guidance on the Operation of the Animals (Scientific Procedures) Act, 1986 (HMSO) and to institutional guidelines.

Hemodynamic stability

Five male Wistar rats (body weights $=432 \pm 24$ g) were anesthetized with isoflurane and the left ventricle cannulated via the right carotid artery using a 1.4F Millar Mikro-tip cannula, especially adapted for use in the rat. Isoflurane was maintained at 1.0–1.5%. Following 15 minutes equilibration (such that stable and reproducible readings were obtained), left ventricular haemodynamic indices, heart rate (HR), left ventricular diastolic pressure (LVDP), left ventricular systolic pressure (LVSP) and rate of change of pressure (dP/dt) were recorded. Measurements were obtained using a pressure transducer attached to the cannula connected to a Powerlab/4SP recorder (ADInstruments, Oxfordshire, United Kingdom). Recordings were made for 10 minutes in the horizontal supine position, after which the animals were tilted into a vertical position (head-up) to simulate conditions in the magnet, for a further 90 minutes. Body temperature was maintained at 37°C throughout.

MR-CINE imaging

Anesthesia was induced in a chamber using 4% isoflurane in 100% oxygen. Animals were positioned supine in a purpose-built rat holder and maintained on 2% isoflurane at 2 L/min oxygen flow throughout the MRI experiments. The cradle was designed for positioning rats vertically in the magnet and comprised an in-built nose cone, lines for the delivery and scavenging of anesthetic gases, temperature control and ECG and respiratory monitoring. Temperature was maintained via warm air that flowed through a home-built heat-exchanger placed within the animal holder and above the coil in the magnet. An ECG and respiratory gating device, developed in-house, was used for monitoring heart and respiration signals (29). ECG signals were obtained from two needles subcutaneously inserted in the fore limbs and respiratory signals from a wire loop loosely fitted on the chest and abdomen of the animals. Rats were secured within the holder using surgical tape, without compressing their abdomen or chest. Additional support for the head was provided by a surgical thread tooth loop attached to the nose-cone. All animals were euthanized after the MRI examinations and their hearts were excised and weighed. Imaging experiments were carried out on an 11.7 T (500 MHz) MR system comprising a vertical magnet (bore size 123 mm—Magnex Scientific, Oxon, United Kingdom), a Bruker Avance console (Bruker Medical, Ettlingen, Germany) and a shielded gradient system (548 mT/m, rise time 160 μs) (Magnex Scientific). A birdcage coil with an inner diameter of 60 mm (Bruker Medical, Ettlingen, Germany) was used to transmit/receive the NMR signals.

The normal high-resolution magnetic resonance cine imaging protocol started with the acquisition of scout images, for the long and short-axis orientation of the heart, using a segmented cardiac-triggered and respiration-gated FLASH-sequence (31). The coil was then tuned and matched, followed by slice-selective shimming and a flip-angle calibration. CINE-MR images were then acquired in nine to ten contiguous slices (slice thickness 1.5 mm) in the short-axis orientation covering the entire heart, using a frame interleaved FLASH imaging sequence. The imaging parameters were: FOV $(51.2 \text{ mm})^2$, matrix size 256×256, TE/TR $= 1.43/4.6$ ms, 17.5° Gaussian excitation pulse. The sequence was ECG-triggered and respiratory gated. Between 28 and 40 frames per heart cycle and two to four phase-encoding steps per respiration cycle were acquired in a segmented fashion (12) resulting in a total experimental time, including experimental preparation of approximately 75 minutes in the vertical position.

Data analysis

Image reconstruction was performed using purpose-written software in Matlab (Mathworks, Natick, Maryland, USA). Raw data were isotropically zero filled by a factor of two and filtered (modified 3rd order Butterworth filter) prior to Fourier transformation, resulting in an in-plane voxel size of 100×100 μm. All image data were exported into TIFF-format and loaded into Scion Image (Scion Corporation, Frederick, Maryland, USA). End-diastolic and end-systolic frames were selected according to maximal and minimal ventricular volumes. In both frames, the epicardial border was outlined first using the free hand drawing function of Scion Image. The LV cavity was then segmented by thresholding. The number of voxels in each compartment multiplied by the pixel size of 0.015 mm^3 yielded the respective volumes. LV mass was obtained by multiplying the volume by the specific gravity of myocardial tissue (1.05 g/cm^3). Based on end-systolic (ESV) and end-diastolic (EDV) volumes, all parameters characterizing cardiac function, such as stroke volume (SV = EDV-ESV), ejection fraction (EF = SV/EDV) and cardiac output (CO = SV $\times$ heart rate) were calculated (12).

Assessment of sequence parameters and gating strategy

To assess the optimum flip angle and gating strategy to be used in subsequent experiments, the following measurements were made on 3 male Wistar rats (body weights = 320 ± 10 g). To measure the flip angle required to optimize the contrast between skeletal muscle, left ventricular myocardium (LVM) and lumen, CINE-MR imaging was performed on a mid-ventricular short axis slice at six different flip angles varying from 5 to 30°. In the post-processed data, the signal to noise ratio (SNR) from a region of interest (ROI) within each tissue type was measured and plotted to indicate the flip angle that provided optimal contrast.

In order to investigate the need for respiration gating at this field strength, cine imaging was performed under various gating and acquisition strategies: ECG gated only (1 average) and ECG and respiratory gated with steady state preparation using 3 heart cycles after each respiratory event (1 average). These strategies were repeated with 4 and 8 averages, respectively, to generate 2 sequences with approximately the same acquisition time for comparison. For all experiments the imaging parameters were as described above.

Validation of technique

To validate and assess the accuracy and reproducibility of CINE-MR imaging in the vertical position, 6 female Wistar rats (body weights = 263 ± 7 g) were imaged using the protocol described above. To assess the reproducibility of our method, segmentation of the high-resolution cine data was performed by two independent observers (DJT and JES) and twice by one observer (DJT).

Cardiac function in a rat model of myocardial infarction

Six male Wistar rats (body weights = 360 ± 20 g) were subjected to myocardial infarction, as described previously (6), and 4 male Wistar rats (body weights = 370 ± 30 g) received sham operations. Anesthesia was induced using 4% isoflurane in 100% oxygen. Rats were intubated and ventilated with 2% isoflurane, 70 breaths per minute, stroke volume 2.5 mL (Hugo-Sachs MiniVent type 845, Harvard Apparatus, Edenbridge, UK). To minimize cardiac arrhythmias, lignocaine (10 mg/kg) was given intramuscularly immediately before surgery, and again two hours after infarction. A thoracotomy was performed in the 4th intercostal space, and a 5/0 Proline suture tied around the left anterior descending coronary artery a few millimetres from its origin (not in the sham operated animals). Subcutaneous buprenorphine (0.2 mg/kg) was given for pain relief, with subcutaneous saline and post-op warming to aid recovery. Eight weeks after infarction, all animals were imaged using the CINE-MR procedure described above.

Statistics

All data were analyzed using single factor ANOVA, and statistical significance was considered at $p < .05$.

RESULTS

Assessment of hemodynamic stability

Figure 1 shows that the LVSP, LVDP, HR and dP/dt were the same in the horizontal position, and at 10, 60 and 90 minutes after the animal was placed in a vertical position. Thus, rat hemodynamics were normal and stable in a vertical position for at least 90 minutes.

MR-CINE imaging technique

Assessment of sequence parameters and gating strategy

Figure 2 shows the normalized signal intensity measurements from the skeletal muscle, left ventricular myocardium and lumen for flip angles between 5 and 30°. The SNR of the lumen was maximal at approximately 25°, the myocardium at between 15 and 20° and the skeletal muscle at approximately 10°.

Figure 3 shows the images acquired with (a) no respiration gating and one average, (b) respiration gating and one average, (c) no respiration gating and 8 averages and (d) respiration gating and 4 averages. The acquisition acquired without respiratory gating (Fig. 3a) showed high levels of periodic image artefact caused by the respiratory motion. This periodic noise was not present in the image acquired with respiratory gating (Fig. 3b), but the image is limited by a low SNR. The images obtained with four and eight repetitions (Figs. 3c & 3d) had low artefact levels and high image quality.

Validation of technique

Figure 4 shows typical mid-ventricular end-diastolic and end-systolic CINE-MR frames from one rat. The image quality and the contrast between myocardium, blood and surrounding tissue allowed easy segmentation of the different regions. In the short-axis images, the left and right ventricular walls could be identified, and the endocardial and epicardial borders were clearly delineated. In the long-axis view, all four heart-chambers and the major thoracic vessels were visible.

Cardiac functional parameters and LV mass measurements are given in Table 1. There was no statistically significant difference between end-diastolic and end-systolic mass. Table 1 also shows that the inter-observer and intra-observer variability for all analyzed parameters was less than 5%, indicating that quantitative analysis of the images was highly reproducible.

Cardiac function in a rat model of myocardial infarction

Figure 5 shows mid-ventricular, end-diastolic, and end-systolic frames from an infarcted rat heart in short and long axis orientations. The arrows in Figures 5b and d indicate wall

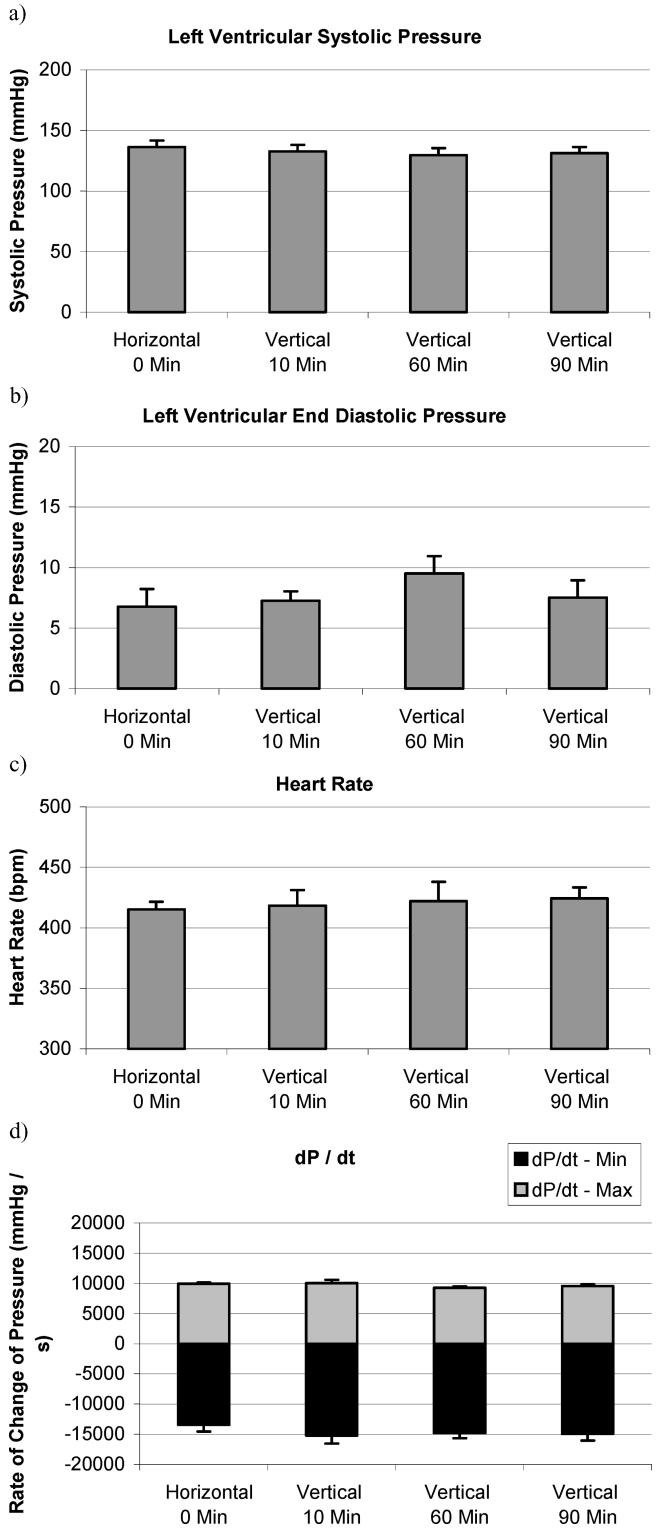

Figure 1. Cardiac hemodynamics : (a) left ventricular systolic pressure, (b) left ventricular diastolic pressure, (c) heart rate and (d) rate of change of developed pressure (dP/dt) in the horizontal position at 0 minutes and in the vertical position at 10, 60 and 90 minutes. Error bars indicate the SEM.

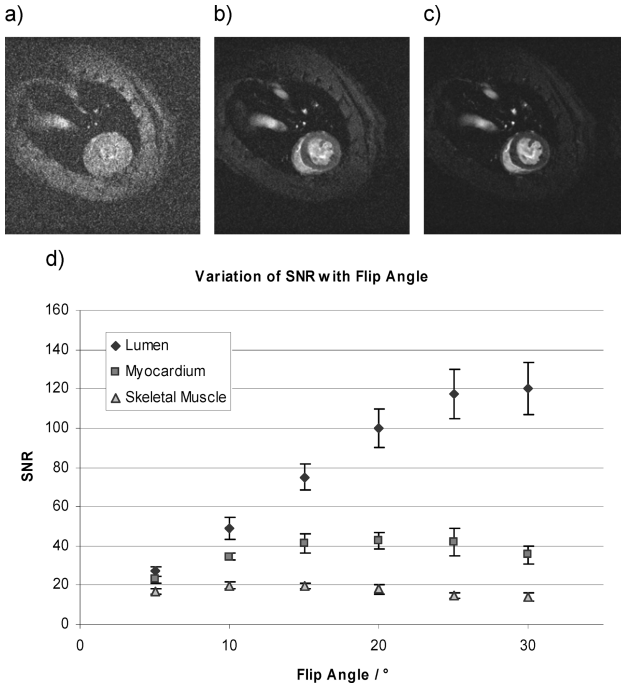

Figure 2. End diastolic short axis images acquired with a flip angle of (a) 5°, (b) 17.5° and (c) 30°. (d) Variation of the acquired signal to noise ratio (SNR) in the cardiac lumen, left ventricular myocardium, and the skeletal muscle at a range of flip angles from 5° to 30°. Error bars indicate the SEM.

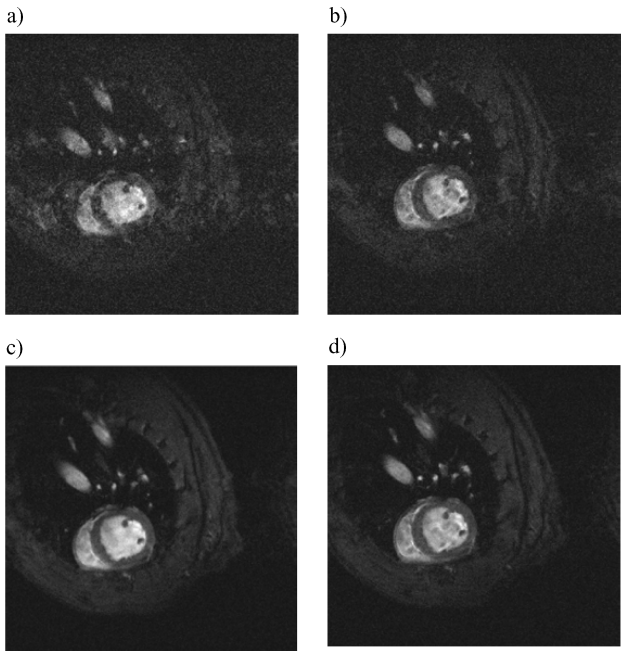

Figure 3. Images obtained under different acquisition strategies; (a) no respiration gating & 1 average, (b) respiration gating & 1 average, (c) no respiration gating & 8 averages and (d) respiration gating & 4 averages.

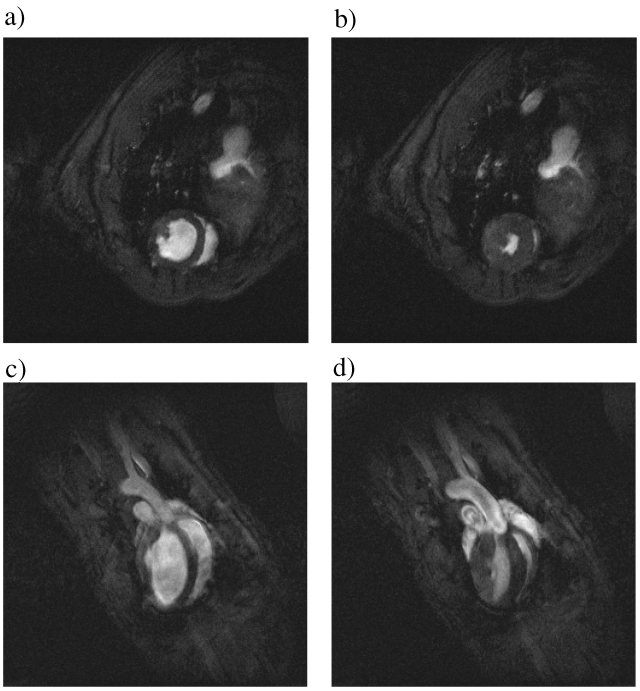

Figure 4. Typical images obtained in a mid ventricular slice of a normal Wistar rat. (a) Short axis orientation at end diastole, (b) short axis orientation at end systole, (c) four chamber long axis orientation at end diastole and (d) four chamber long axis orientation at end systole.

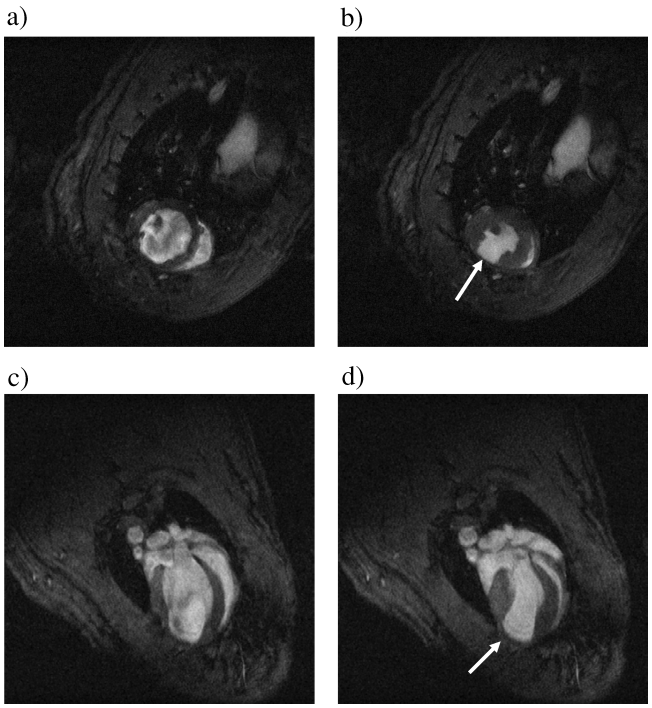

Figure 5. Typical image quality obtained in a mid ventricular slice of an infarcted Wistar rat heart, 8 weeks after infarction. (a) Short axis orientation at end diastole, (b) short axis orientation at end systole, (c) four chamber long axis orientation at end diastole and (d) four chamber long axis orientation at end systole. White arrows indicate the region of infarction.

thinning in the infarcted region of the left ventricle. These images show reduced myocardial contraction in systole and left ventricular dilation in diastole. Quantitative analysis, shown in Table 2, revealed a 2.8 fold increase in the systolic volume, leading to an 18% reduction in the ejection fraction of the infarcted hearts. However, the cardiac output was the same for all hearts due to an increase in the end diastolic volume in the infarcted hearts.

Table 1. Cardiac parameters measured in normal rats and inter-observer and intra-observer variability measurements

	Measured Parameters	Inter-Observer Variability (%)	Intra-Observer Variability (%)
Body Weight (g)	263 ± 7	—	—
End Diastolic Weight (mg)	518 ± 15	3.1 ± 0.7	3.9 ± 1.0
End Systolic Weight (mg)	541 ± 21	4.5 ± 0.9	3.9 ± 1.1
End Diastolic Volume (μL)	291 ± 16	2.4 ± 0.6	2.9 ± 0.6
End Systolic Volume (μL)	59 ± 6	4.6 ± 1.2	3.4 ± 1.0
Stroke Volume (μL)	232 ± 17	4.2 ± 0.8	4.0 ± 0.8
Ejection Fraction (%)	80 ± 2	1.8 ± 0.5	1.5 ± 0.3
Heart Rate (bpm)	354 ± 10	—	—
Cardiac Output (mL/min)	82 ± 5	—	—
Heart to Body Weight Ratio ($\times 10^{-3}$)	1.97 ± 0.06	—	—

Values are means $\pm$ SEM.

DISCUSSION

We have found that rats are hemodynamically stable positioned vertically for up to 90 minutes, which has allowed the

Table 2. Cardiac parameters measured in normal and infarcted rats

	Sham Operated Animals (n = 4)	Infarcted Animals (n = 6)
Body Weight (g)	371 ± 26	360 ± 24
End Diastolic Weight (mg)	624 ± 39	707 ± 23
Heart to Body Weight Ratio ($\times 10^{-3}$)	1.69 ± 0.03	2.01 ± 0.14
End Diastolic Volume (μl)	309 ± 21	407 ± 18*
End Systolic Volume (μl)	50 ± 4	138 ± 21*
Stroke Volume (μl)	259 ± 19	270 ± 28
Ejection Fraction (%)	84 ± 1	66 ± 5*
Heart Rate (bpm)	399 ± 3	379 ± 5*
Cardiac Output (μl/min)	103 ± 7	102 ± 9

*$p < .05$, Values are means $\pm$ SEM.

use of an 11.7T vertical bore MR system to acquire accurate and reproducible measurements of rat cardiac structure and function. We examined several acquisition strategies and developed a protocol that allowed data acquisition at a high spatial and temporal resolution.

The ability to use high-field, vertical bore experimental MR systems for monitoring cardiac function in rats depends on the vertical position not altering the animal's normal physiology. The hemodynamic stability experiments demonstrated that there was no alteration in rat cardiac pressures or heart rate when placed in a vertical position for up to 90 minutes. Thus, rats can be positioned vertically for cardiac MR imaging over the ~75 minutes required for the imaging protocol. This could allow the direct comparison of structural and functional information from *in vivo* imaging and energetic information from *in vivo* or isolated perfused heart ^{31}P spectroscopy experiments.

We have used our vertical bore system to measure cardiac structure and function in mice (12), but new problems were encountered in the acquisition of the ECG signals when imaging rats due to magnetohydrodynamic effects (30). The large volume of blood, an electrically conductive fluid, flowing in the rat aorta was sufficient to induce detectable voltages in the ECG electrodes in the high magnetic field. These induced voltages often obscured the ECG. To overcome this problem, we modified the ECG detection hardware to selectively filter, via differences in frequency, the ECG signal to yield either the ECG or blood-flow induced signal. This provided the option of two separate gating signals, both related to cardiac activity, although with a temporal delay between them, from which we could trigger the acquisition.

The contrast in bright-blood cine imaging is based on the difference in the signals from the unsaturated magnetization of the blood flowing into the imaging slice from the saturated magnetization of stationary tissues within the imaging slice. The contrast between the left ventricular myocardium and the lumen depended on the flip-angle and the repetition time. In our experiments, the repetition time was minimized to yield the highest temporal resolution and the flip angle varied to provide the optimum image contrast. The maximum contrast between the left ventricular myocardium and the lumen was found to be at 25–30° (Fig. 2c). Such flip angles would maximize the contrast solely for cardiac function. However, should the measurement of left ventricular mass be required, a lower flip-angle would be better because the SNR of the myocardial tissue is higher. In our experiments, a flip angle of 17.5° (Fig. 2b) gave reasonable contrast between blood and myocardium and provided the maximum SNR in the myocardium.

Our previous work in mice at this field strength showed that the use of respiratory gating was essential to enable the acquisition of artifact free CINE-MR images (12). However, isoflurane anesthesia causes mice to breathe impulsively ("snatch-breathing"), which minimizes the time within a respiratory cycle used for breathing, but increases the motional amplitude. We have not observed this respiration in Wistar rats, in which respiration was shallower and faster than in mice. Consequently, the need for respiration gating was examined using several different acquisition strategies.

The single average acquisition with no respiratory gating showed significant artifacts that were not present in the single average respiratory-gated acquisition. However, due to the low sensitivity of the RF probe, the quality of a single averaged image was not sufficient for quantification, so averaging was included in the acquisition scheme to improve the SNR of the acquired images. It was found that, at the normal rat heart and respiration rates, it was possible to acquire eight averages of the non-gated images in the same time as four averages of the respiratory gated images. Figure 3(c–d) shows that for both the gated and non-gated cases; the image quality was high. There was still some low level periodic artifact in the non-gated images, but the additional averages that could be achieved in the same acquisition time meant that the image quality was acceptable for both acquisition schemes. Thus, in contrast to mice, there was no clear requirement for respiratory gating in Wistar rats and an acquisition strategy yielding the best image quality in the shortest acquisition time was the best option. Normally respiration gating was used; however, animals with a fast respiration rate (>60 per minute) or a slow heart rate (<300) were imaged without respiratory-gating due to the decreased number of ECG's that could be used between successive respiration events.

Figure 4 demonstrates the image quality obtained with the MR protocol described. The temporal resolution was nearly twice as fast as previously reported (Nahrendorf et al., 2001), and the experimental image resolution of 200 × 200 μm in-plane also exceeded reported values by 15–35% (15). The high reproducibility of the technique was demonstrated by <5% inter-observer and intra-observer variability. Figure 5 demonstrates that it was possible to acquire high quality images in a rat model of cardiac infarction, enabling infarcted tissue and the function to be determined easily and accurately.

CONCLUSION

In conclusion, rat hemodynamics were stable in the vertical position for at least 90 minutes, which allowed cardiac imaging in a high-field MR system with higher temporal and spatial resolution than previously reported. A flip angle of approximately 17.5° was found to provide good contrast between the left ventricular myocardium and lumen, whilst maximizing the SNR of the myocardial tissue. Although it reduced periodic artifact levels, respiratory gating was not essential for high quality, low artifact level CINE-MR images. Structure and function in normal and infarcted rat hearts could be measured with high accuracy and reproducibility, demonstrating that MR systems with a vertical bore can be used to image the *in vivo* rat heart.

REFERENCES

1. Braunwald E. Shattuck lecture—cardiovascular medicine at the turn of the millennium: Triumphs, concerns, and opportunities. New England Journal of Medicine 1997;337:1360–9.

2. Hellermann JP, Jacobsen SJ, Gersh BJ, Rodeheffer RJ, Reeder GS, Roger VL. Heart failure after myocardial infarction: A review. American Journal of Medicine 2002;113:324–30.
3. Franco F, Dubois SK, Peshock RM, Shohet RV. Magnetic resonance imaging accurately estimates lv mass in a transgenic mouse model of cardiac hypertrophy. American Journal of Physiology-Heart and Circulatory Physiology 1998;43:H679–83.
4. Franco F, Thomas GD, Giroir B, Bryant D, Bullock MC, Chwialkowski MC, et al. Magnetic resonance imaging and invasive evaluation of development of heart failure in transgenic mice with myocardial expression of tumor necrosis factor-alpha. Circulation 1999;99:448–54.
5. Kubota T, McTiernan CF, Frye CS, Slawson SE, Lemster BH, Koretsky AP, et al. Dilated cardiomyopathy in transgenic mice with cardiac-specific overexpression of tumor necrosis factor-alpha. Circulation Research 1997;81:627–35.
6. Lygate CA, Hulbert K, Monfared M, Cole MA, Clarke K, Neubauer S. The ppar gamma-activator rosiglitazone does not alter remodeling but increases mortality in rats post-myocardial infarction. Cardiovascular Research 2003;58:632–7.
7. Sidell RJ, Cole MA, Draper NJ, Desrois M, Buckingham RE, Clarke K. Thiazolidinedione treatment normalizes insulin resistance and ischemic injury in the zucker fatty rat heart. Diabetes 2002;51:1110–7.
8. Wilding JR, Schneider JE, Sang AE, Davies KE, Neubauer S, Clarke K. Dystrophin- and mlp-deficient mouse hearts: Marked differences in morphology and function, but similar accumulation of cytoskeletal proteins. Faseb Journal 2004;18:U303–2.
9. Williams SP, Gerber HP, Giordano FJ, Peale FV, Bernstein LJ, Bunting S, et al. Dobutamine stress cine-mri of cardiac function in the hearts of adult cardiomyocyte-specific vegf knockout mice. Journal of Magnetic Resonance Imaging 2001;14:374–82.
10. Gilson WD, Yang ZQ, French BA, Epstein FH. Measurement of myocardial mechanics in mice before and after infarction using multislice displacement-encoded mri with 3d motion encoding. American Journal of Physiology-Heart and Circulatory Physiology 2005;288:H1491–7.
11. Nahrendorf M, Hiller KH, Hu K, Ertl G, Haase A, Bauer WR. Cardiac magnetic resonance imaging in small animal models of human heart failure. Medical Image Analysis 2003;7:369–75.
12. Schneider JE, Cassidy PJ, Lygate C, Tyler DJ, Wiesmann F, Grieve SM, et al. Fast, high-resolution in vivo cine magnetic resonance imaging in normal and failing mouse hearts on a vertical 11.7 t system. Journal of Magnetic Resonance Imaging 2003;18:691–701.
13. Constantino G, Shan K, Flamm SD, Sivananthan MU. Role of MRI in clinical cardiology. Lancet 2004;363:2162–71.
14. Nahrendorf M, Wiesmann F, Hiller KH, Hu K, Waller C, Ruff J, et al. Serial cine-magnetic resonance imaging of left ventricular remodeling after myocardial infarction in rats. Journal of Magnetic Resonance Imaging 2001;14:547–55.
15. Bove CM, Yang ZQ, Gilson WD, Epstein FH, French BA, Berr SS, et al. Nitric oxide mediates benefits of angiotensin ii type 2 receptor overexpression during post-infarct remodeling. Hypertension 2004;43:680–5.
16. Chapon C, Franconi F, Lemaire L, Marescaux L, Legras P, Saint-Andre JP, et al. High field magnetic resonance imaging evaluation of superparamagnetic iron oxide nanoparticles in a permanent rat myocardial infarction. Investigative Radiology 2003;38:141–6.
17. Crowley JJ, Huang CLH, Gates ARC, Basu A, Shapiro LM, Carpenter TA, et al. A quantitative description of dynamic left ventricular geometry in anaesthetized rats using magnetic resonance imaging. Experimental Physiology 1997;82:887–904.
18. Jones JR, Mata JF, Yang ZQ, French BA, Oshinski JN. Left ventricular remodeling subsequent to reperfused myocardial infarction: Evaluation of a rat model using cardiac magnetic resonance imaging. Journal of Cardiovascular Magnetic Resonance 2002;4:317–26.
19. Nahrendorf M, Hiller KH, Greiser A, Kohler S, Neuberger T, Hu K, et al. Chronic coronary artery stenosis induces impaired function of remote myocardium: Mri and spectroscopy study in rat. American Journal of Physiology-Heart and Circulatory Physiology 2003;285:H2712–21.
20. Nahrendorf M, Hu K, Fraccarollo D, Hiller KH, Haase A, Bauer WR, et al. Time course of right ventricular remodeling in rats with experimental myocardial infarction. American Journal of Physiology-Heart and Circulatory Physiology 2003;284:H241–8.
21. Nahrendorf M, Wiesmann F, Hiller KH, Han H, Hu K, Waller C, et al. In vivo assessment of cardiac remodeling after myocardial infarction in rats by cine-magnetic resonance imaging. Journal of Cardiovascular Magnetic Resonance 2002;2:171–80.
22. Rehwald WG, Reeder SB, McVeigh ER, Judd RM. Techniques for highspeed cardiac magnetic resonance imaging in rats and rabbits. Magnetic Resonance in Medicine 1997;37:124–30.
23. Saeed M, Watzinger N, Krombach GA, Lund GK, Wendland MF, Chujo M, et al. Left ventricular remodeling after infarction: Sequential mr imaging with oral nicorandil therapy in rat model. Radiology 2002;224:830–7.
24. Schalla S, Wendland MF, Higgins CB, Ebert W, Saeed M. Accentuation of high susceptibility of hypertrophied myocardium to ischemia: Complementary assessment of gadophrin-enhancement and left ventricular function with MRI. Magnetic Resonance in Medicine 2004;57:552–8.
25. Waller C, Hiller KH, Kahler E, Hu K, Nahrendorf M, Voll S, et al. Serial magnetic resonance imaging of microvascular remodeling in the infarcted rat heart. Circulation 2001;103:1564–9.
26. Wise RG, Huang CLH, Al-Shafei AIM, Carpenter TA, Hall LD. Geometrical models of left ventricular contraction from mri of the normal and spontaneously hypertensive rat heart. Physics in Medicine and Biology 1999;44:2657–76.
27. Wiesmann F, Neubauer S, Haase A, Hein L. Can we use vertical bore magnetic resonance scanners for murine cardiovascular phenotype characterization? Influence of upright body position on left ventricular hemodynamics in mice. Journal of Cardiovascular Magnetic Resonance 2001;3:311–5.
28. Loeppky JA. Cardiorespiratory responses to orthostasis and the effects of propranolol. Aviat Space Environ Med 1975;46:1164–9.
29. Cassidy PJ, Schneider JE, Grieve SM, Lygate C, Neubauer S, Clarke K. Assessment of motion gating strategies for mouse magnetic resonance at high magnetic fields. Journal of Magnetic Resonance Imaging 2004;19:229–37.
30. Chakeres D, Kangarlu A, Boudoulas H, Young D. Effect of static magnetic field exposure of up to 8 tesla on sequential human vital sign measurements. Journal of Magnetic Resonance Imaging 2003;18:346–52.
31. Haase A, Frahm J, Matthaei D, Hanicke W, Merboldt KD. Flash imaging—rapid nmr imaging using low flip-angle pulses. Journal of Magnetic Resonance 1986;67:258–66.